Desalination and Water Treatment
www.deswater.com

doi:10.5004/dwt.2018.22437

115 (2018) 115–125
May

Optimization of process parameters for the adsorption of nickel onto activated carbon using response surface methodology

J.B. Mathangi, M. Helen Kalavathy*

Department of Chemical Engineering, A.C.Tech, Anna University, Chennai, Tamil Nadu, India, email: jbmathangi@gmail.com (J.B. Mathangi), Tel. +91-9884694251, email: helenkalavathy@gmail.com (M.H. Kalavathy)

Received 15 February 2017; Accepted 26 February 2018

ABSTRACT

In the present study, the adsorption characteristics of Ni^{2+} onto activated carbon produced from the biomass residue *Citrullus colocynthis* peel was studied. Batch experiments were conducted to remove Ni^{2+} from synthetic solutions. Effects of various operating parameters such as pH, contact time, activated carbon loading and initial Ni^{2+} ion concentration on the adsorption process of Ni^{2+} have been studied. Kinetic and isotherm studies for the removal of Ni^{2+} from synthetic wastewater were carried out. Langmuir isotherm model fits to the adsorption of Ni^{2+} ion onto activated carbon sourced from CCP. The pseudo-second-order model was found to explain the kinetics of Ni^{2+} adsorption most effectively. The optimization of the process was carried out by using central composite rotary design in response surface methodology.

Keywords: Adsorption; Ni^{2+}; Response surface methodology; Kinetics; Isotherms; Central composite rotary design

1. Introduction

Pollution today has become accelaratively prevalent in our day today lives and it has a fairly negative impact on our health. Out of all the pollutants, heavy metals are important part which should never be neglected. With increase in the number of industries, developing society and the advancement in technology heavy metals, dyes, organic substances and other such toxic pollutants are let out into the water bodies [1]. Heavy metals have proneness to bio-accumulate and thereby enter the food chain ending up as a permanent addition to the environment [2]. The removal of heavy metals from waste water has become the subject of significant interest owing to inflexible legislations introduced to control water pollution. Mercury, chromium, cadmium, nickel, arsenic, lead, beryllium, selenium and manganese are a few of the metals called ‘heavy’ because of their high relative atomic mass which can get retained in nature and can cause damage even at very low concentrations. Ni^{2+} used in industrial processes viz. storage battery industries; silver refineries and zinc based castings are carried by air and water and are discharged into the environment. Excess discharge of this heavy metal into the environment is a serious issue as human’s exposure to Ni^{2+} causes headache, dermatitis, dizziness, dry cough, nausea, vomiting, renal damage, nervous disabilities, chest pain, cancer in lungs, nose, bones, etc. In general it is listed as carcinogenic for all living organisms. International laws have been enforced by World Health Organization (WHO) and Euro Environmental Contracts (EEC) and have set standards for the concentration of its discharge into surface waters at 0.02 mg L^{-1} [3]. The conventional techniques which are frequently used for the removal of Ni^{2+} from the industrial effluents are physical-chemical methods, such as chemical precipitation, evaporative recovery, filtration, membrane technologies, electrochemical treatment and ion exchange [4–6]. These processes may be expensive or ineffective. The high cost of treatment and the issues related to the operation processes lead for finding out some newer methods. Biological methods such as biosorption/bioaccumulation may provide a striking alternative to physical-chemical methods for the elimination of heavy

---

*Corresponding author.

1944-3994 / 1944-3986

metals. Of all these methods mentioned for the removal of Ni^{2+}, coagulation, precipitation and reduction methods have been adopted industrially, however, with the disadvantage of giving out huge amount of sludge and have low efficiencies. Ion-exchange and reverse osmosis, although effective are expensive. Hence cheaper and more viable alternatives are being considered of which adsorption is one [7,8]. It may be observed that few unconventional and less expensive adsorbents have been investigated for the production of activated carbon. The precursors such as moss peat [9], coconut husk [10], chitosan [11], coir pith, rice husk [12], tea leaves [13], almond husk [14], Manihot Esculenta peel, Hemp jung shell, Delonix regia shell and Aegle marmelos shell [15], tamarind wood [16], shells of Macore fruit [17] have been investigated for the removal of toxic metals from aqueous solutions. In this work activated carbon (AC) produced from the biomass residue *Citrullus colocynthis* peel (CCP) by chemical activation was studied as a possible route to adsorb Ni from synthetic waste water. The optimization was carried out using response surface methodology (RSM). RSM focuses at the development of a mathematical model to describe the effects, relationships of the main process variables and to maximize the adsorption.

2. Experimental procedure

2.1. Materials and methods

2.1.1. Reagents

A.R grade Nickel sulphate supplied by Central Drug House Private Limited, India was used. Nickel sulphate solution of 1000 mg L^{-1} was prepared by dissolving Nickel sulphate in distilled water. Solutions for working were then prepared for the required concentrations by dilution. The other chemicals such as dimethylene glyoxime, iodine, sodium citrate, sulphuric acid used for the analysis of Ni^{2+} were procured from Sisco Research Laboratories Pvt. Ltd., India and they were of analytical grade.

2.1.2. Preparation of adsorbent

Citrullus colocynthis peel for the preparation of AC was procured from Tuticorin (Tamilnadu, India). The precursor CCP was impregnated with phosphoric acid in 1:1.5 ratio and kept for 24 h, so that the reagents are fully adsorbed into the raw material. After impregnation, the mixture was transferred to a Pyrex glass plate and placed in the hot air oven for drying at 110ºC for 1.5 h. After drying, the precursors were activated in a self-generated atmosphere at 400ºC in a muffle furnace for an hour. The carbon thus produced was then repeatedly washed with distilled water to recover all the excess acid. AC thus obtained was dried in a hot air oven at a temperature of 105 ± 5°C until a constant weight of AC was reached [18]. AC was sieved for particle size of 2–5 mm and stored in a tight lid container for further adsorption studies.

2.1.3. Characterization of CCP

The activated CCP produced was subjected to proximate analysis in order to test it for properties like moisture content, ash content, volatile content, fixed carbon, charcoal yield and bulk density. The characteristics such as iodine number, methylene blue number, methyl violet number, pore volume, surface area and pH_{ZPC} were also found out.

2.1.4. Adsorption experiments

Adsorption experiments were carried out by agitating the AC in 100 mL of Ni^{2+} ion solution of desired concentration and pH, in an orbitary shaker at 150 rpm. Adsorption experiments were carried out in conical flasks of capacity 250 mL. Each flask was filled with 100 mL of adsorbate solution which was varied from 10 to 30 mg L^{-1}. The adsorbent loading ranged between 0.1 and 0.5 g (100 mL $^{-1}$) of sample solution. All experiments were conducted using double distilled water. The samples were taken at different time intervals (30–150 min) and analysed for Ni concentration using a UV-Vis spectrophotometer by forming a complex with dimethylglyoxime at 470 nm. The experiments were carried out by varying carbon loading, initial Ni ion concentration, contact times, and pH. The pH of the Ni^{2+} ion solutions were varied by using HCl and NaOH for the study of the effect of pH. The adsorption capacity was calculated using:

$$q_e = \frac{\left[(C_o - C_e)V\right]}{M} \tag{1}$$

where C_o is the initial Ni^{2+} ion concentration in the solution (mg L^{-1}), C_e is the concentration of Ni^{2+} ion in the solution at equilibrium time (mg L^{-1}), V is the volume of the solution (L) and M is the mass of the adsorbent (g).

2.1.5. Response surface methodology

Being economical for extracting the maximum amount of complex information, reduction in experimental time thereby saving operational and personnel cost are the essential characteristics for an experimental design methodology [19]. This requirement is precisely met with the help of response surface methodology (RSM). By keenly designing the experiments, the aim is to optimize an output parameter which is affected by many non-dependent input parameters. Runs, which represents the series of tests which is used to make changes in the input parameters in order to find the reason for changes in the output response. This method is a multivariate non-linear model which is widely applied to optimize variables in adsorption process [20–22]. Its main applications include the realization of the interaction between variables and their aggregate effect on the whole process. Thus RSM can be used for optimization of separation processes with minimum number of experimental runs based on the planned experimental design [23].

2.1.6. Experimental design using central composite rotary design

Experimentation was done using central composite design which incorporates four variable calculations. The variance of the predicted response Y is designed to minimize the large number of experiments required to essentially find the response values. The distance from the Centre of the design is established by a function X, and coordinates of the point on the response surface used to find the standard error is signified by the coefficient β [24–27]. The number of points in the factorial portion of the design for rotatability is the value α, which is given by

$$\alpha = (F)^{¼} \tag{2}$$

F is the number of points where $F = (2)^{K}$ (*k* denotes the number of factors in the cube portion of the design). Since $K = 4$ we have $F = (2)^{K} = 16$ points where α = 2 from above equation. Tables 1 and 2 show the levels of variables considered for CCRD and the coded and actual variables used in the CCRD respectively.

$$x_i = \frac{\alpha\left[2X_i - \left(X_{max} - X_{min}\right)\right]}{\left[X_{max} - X_{min}\right]} \tag{3}$$

where x_i is the dimensionless coded value of the i^{th} variable, X_i the natural value of the i^{th} variable respectively. Once the desired range of variables is defined, they are coded to lay at factorial points of ± 1 and ± α for axial points of ± α. The matrix contains two-level full factorial design, six centre points, eight axial points and 16 fact points. Experiments were conducted using these sets (Tables 1 and 2) to observe the responses while validating the single-response model of the adsorption process. The sequence of experiments was randomized to prevent the effects of uncontrolled factors.

2.2. Statistical methods

From the regression of the responses, a second order polynomial equation was considered for all the experimental data:

$$Y_i = \beta_0 + \sum_i \beta_i x_i + \sum_{ii} \beta_{ii} x_i^2 + \sum_{ij} \beta_{ij} x_i x_j \tag{4}$$

where Y_i is the predicted response, $x_i x_j$ are the independent variables, β_i is the i^{th} linear variable coefficient, *and* β*ij* is the *ij*th interaction coefficient.

$$Y = \beta_0 + \beta_1 A + \beta_2 B + \beta_3 C + \beta_4 D + \beta_{11} A^2 + \beta_{22} B^2 + \beta_{33} C^2 + \beta_{44} D^2 + \beta_{12} AB + \beta_{13} AC + \beta_{14} AD + \beta_{23} BC + \beta_{24} BD + \beta_{34} \tag{5}$$

where $\beta_0, \beta_1, \beta_2, \beta_3, \beta_4, \beta_{11}, \beta_{22}, \beta_{33}, \beta_{44}, \beta_{12}, \beta_{13}, \beta_{14}, \beta_{23}, \beta_{24}, \beta_{34}$ are the regression coefficients, A, B, C and D are the coded independent variables and Y is the particular response evaluated. For the optimization process, the counter plots were plotted using these values [28].

Table 2
Independent variables and result for the adsorption of nickel ion by central composite rotary design

Run order	Standard order	Coded variables				Actual variables			
		A	B	C	D	A	B	C	D
1	2	–1	1	–1	–1	0.2	25	4	60
2	1	1	–1	–1	–1	0.4	15	4	60
3	10	0	0	0	0	0.3	20	6	90
4	8	–1	1	1	1	0.2	30	8	120
5	5	–1	–1	–1	1	0.2	25	4	120
6	4	1	1	1	–1	0.4	15	8	60
7	6	1	1	–1	1	0.4	25	4	120
8	3	–1	–1	1	–1	0.2	15	8	60
9	7	1	–1	1	1	0.4	15	8	120
10	9	0	0	0	0	0.3	20	6	90
11	26	0	0	2	0	0.3	20	10	90
12	29	0	0	0	0	0.3	20	6	90
13	27	0	0	0	–2	0.3	20	6	30
14	21	–2	0	0	0	0.1	20	6	90
15	23	0	–2	0	0	0.3	10	6	90
16	22	2	0	0	0	0.5	20	6	90
17	28	0	0	0	2	0.3	20	6	150
18	30	0	0	0	0	0.3	20	6	90
19	24	0	2	0	0	0.3	30	6	90
20	25	0	0	–2	0	0.3	20	2	90
21	11	–1	–1	–1	–1	0.2	15	4	60
22	15	1	–1	–1	1	0.4	15	4	120
23	16	–1	1	–1	1	0.2	25	4	120
24	14	–1	1	1	–1	0.2	25	8	60
25	12	1	1	–1	–1	0.4	25	4	60
26	20	0	0	0	0	0.3	20	6	90
27	13	1	–1	1	–1	0.4	15	8	60
28	19	0	0	0	0	0.3	20	6	90
29	17	–1	–1	1	1	0.2	15	8	120
30	18	1	1	1	1	0.4	25	8	120

Table 1
Level of variables considered for the adsorption of nickel ion by central composite rotary design

S. No	Variables	Parameter	Variable level				
			–2 (–α)	–1	0	+1	2 (+α)
1	A	Carbon loading (g (100 mL)$^{-1}$)	0.1	0.2	0.3	0.4	0.5
2	B	Initial Ni concentration (mg L^{-1}).	10	15	20	25	30
3	C	pH	2	4	6	8	10
4	D	Time (min)	30	60	90	120	150

2.3. RSM evaluation

The model was designed and prepared using various statistical methods which were used to review the experimental error, and to find the viability of the model using a dedicated RSM program. The capability of the Statistical model was justified using analysis of variance (ANOVA). While choosing the models, care must be taken to ensure that the subsets with fewer terms are selected to ensure that they can be a good representation of the validated data. The concluding optimized polynomial equation can be used to picture the relationship between the variables by three dimensional surface plots or contour plots. They aid in seeing the relative influence of parameters, to find an optimum parameter combination, and to predict experimental results for other parameter combinations [29].

3. Results and discussion

3.1. Proximate analysis

The moisture content, ash content, volatile matter, fixed carbon, yield, particle size and bulk density of the CCP was found out and results are shown in Table 3. The moisture content, ash content and volatile matter content are low which gave rise to the fixed carbon content of 56.6%. As CCP is woody material, its final yield % is also high when compared to the lignocellulosic material which is an added advantage using CCP as precursor for adsorption. The particle size was found to be 0.072 mm. As batch adsorption studies are carried out, powdered AC will be more effective than the granular carbon as it has larger surface area available for adsorption to take place.

3.2. Characterization of CCP

Table 4 shows the iodine, methylene blue, methyl violet number, pore volume, BET surface area and pH_{ZPC} obtained. From the Table 4 it can be concluded that the characteristics of the prepared CCP adsorbent is comparatively better and economical than the commercially available AC. The methylene blue and methyl violet number are low than the iodine number and the iodine number corresponds to the micro pores. From Table 4 it can be inferred that the iodine number for CCP is higher than the commercial AC. As the ionic radius of Ni^{2+} is 0.69 Å which is closer to the range of micro pores (< 2 nm) it is very much sufficient for the adsorption to take place. And if suppose the pores are larger than 2 nm desorption would also take place simultaneously which is not the case in the present study. So this proves that the adsorption process will be more effective and efficient with CCP [30].

Table 3
Proximate analysis of activated CCP

Parameters	CCP
Moisture content (%)	8.12
Volatile matter content (%)	25.34
Ash content (%)	9.94
Fixed carbon (%)	56.6
Yield (%)	52.3
Partial size (mm)	0.074
Bulk density (g/cc)	0.33

3.3. Effect of contact time

Contact time studies were carried out at 30ºC and pH of 6 with 0.3 g (100 mL)$^{-1}$ of the carbon loading for 20 mg L^{-1} initial Ni ion concentrations at different time intervals (Fig. 1). It was seen that the adsorption capacity of AC increased with contact time and attained maximum value at 150 min. It was also noted that any further increase in the contact time did not show a significant change in the adsorption capacity. Hence the equilibrium time was taken as 150 min. Therefore, the time taken for attaining equilibrium was set at 150 min in further studies.

3.4. Effect of initial Ni^{2+} ion concentration

Experiments were carried out for different initial Ni ion concentrations at a fixed carbon loading 0.3 g (100 mL)$^{-1}$, pH 6, temperature 30°C and at a time 150 min (Fig. 2). The adsorption capacity was seen to increase with increase in initial Ni ion concentration due to enhanced driving force

Table 4
Characteristics of adsorbents

Characteristics of adsorbents	Characteristic value	
	CCP	Commercial AC
Iodine number (mg/g)	924.35	834
Methylene blue (mg/g)	125	210
Methyl violet (mg/g)	113	125
Pore volume (cm^3/g)	0.61	0.3187
BET Surface area (m^2/g)	721.48	482.21
pH_{ZPC}	6.01	6.67

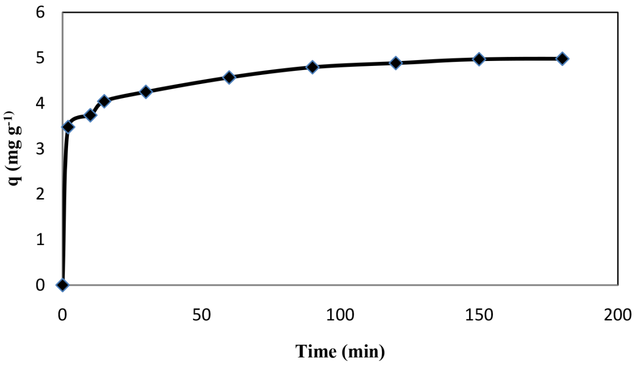

Fig. 1. Effect of contact time on adsorption capacity (Carbon loading = 0.3 g (100 mL)$^{-1}$, Initial Ni ion concentration = 20 mg L^{-1}, Adsorption temperature = 30ºC, pH = 6).

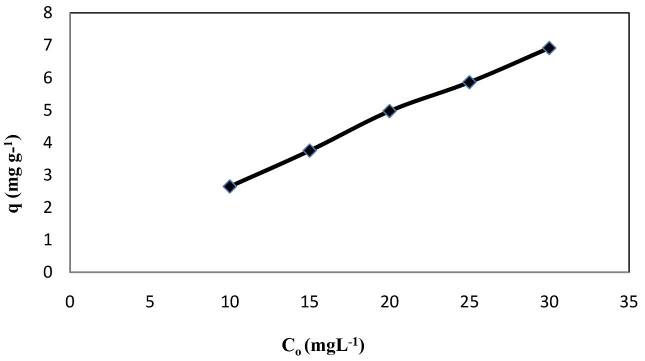

Fig. 2. Effect of initial Ni ion concentration (carbon loading = 0.3 g (100 mL)$^{-1}$, adsorption temperature = 30ºC, pH = 6, Time = 150 min).

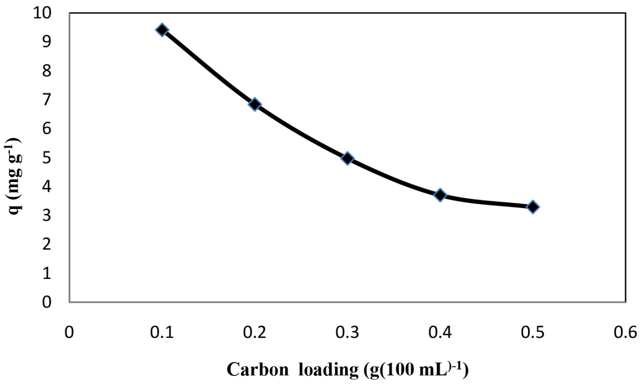

Fig. 3. Effect of carbon loading (initial Ni ion concentration = 20 mg L^{-1}, adsorption temperature = 30ºC, pH = 6, time = 150 min)

[20,31,32]. The values of adsorption capacity increased from 4.97 mg g^{-1} to 7.69 mg g^{-1} when the metal ion concentration was increased from 10 mg L^{-1} to 30 mg L^{-1}.

3.5. Effect of carbon loading

The effect of AC loading on adsorption capacity was studied in order to determine the necessary AC quantity required for the optimal removal of Ni^{2+} ions. The adsorption studies were carried out at a pH of 6, temperature of 30ºC for different retention periods taking 100 mL of 20 mg L^{-1} of nickel sulphate solution for various loadings of AC (Fig. 3). It was inferred that the adsorption capacity of AC decreased from 9.39 mg g^{-1} to 3.42 mg g^{-1} when the weight of AC was increased from 0.1 g (100 mL)$^{-1}$ to 0.5 g (100 mL)$^{-1}$. This behaviour is because of the fact that more the AC, greater will be the availability of the exchangeable sites or surface offered to the adsorption of Ni^{2+} ions [18].

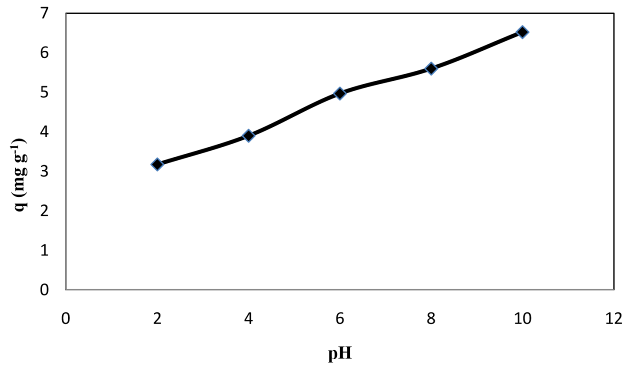

Fig. 4. Effect of pH (carbon loading = 0.3 g (100 mL)$^{-1}$, initial Ni ion concentration = 20 mg L^{-1}, adsorption temperature = 30ºC , time = 150 min).

3.6. Effect of pH

Experiments were carried out to study the effects of pH at temperature of 30°C by varying the initial pH of Ni^{2+} solution from 2 to 10 for a constant carbon loading of 0.3 g (100 mL)$^{-1}$ of the solution (Fig. 4). The experiments were conducted for equilibration time previously determined. The removal of Ni^{2+} ions was found to increase with increasing pH till 10 for 20 mg L^{-1}. From Fig. 4, the removal of Ni^{2+} ions was found to increase with increasing pH till 10. It is extensively reported that Ni^{2+} exists as predominant species till pH 7 and at higher pH several hydroxides starts precipitating [33]. A typical aqueous solution of nickel ions, where pH at which the nickel cation dissociates to form the proton (i.e. at which the solution will have an excess of OH^{-} ions) which can cause precipitation of NiOH indicatively has the value in the range 7.5–10. The increase in the adsorption depends on the properties of the adsorbent surface and Ni ion. The increase in the adsorption capacity with pH is due to the increase in the negative charge on the carbon surface. Though the adsorption capacity increased above pH 6, the proper reason behind it was not concluded whether it is solely due to adsorption or by precipitation. Hence, further reconfirmation was done by carrying out the pH$_{ZPC}$ studies by varying the pH range from 2–10. The point of zero charge is the pH at which the surface of the adsorbent is neutral, i.e., contains as much positively charged as negatively charged surface functions. Below this value, the surface is positively charged; beyond this value, it is negatively charged. So normally, it is always easier to adsorb a cation on a negatively charged surface, and an anion on a positively charged surface. In pH$_{ZPC}$, it was concluded that visible precipitation was observed above pH 6. For this reason, further metal sorption studies were carried at an optimum pH value of 6 because precipitation of nickel hydroxide was observed at a pH greater than 6.

4. Adsorption isotherm

Adsorption isotherm studies are usually carried out with Langmuir and Freundlich isotherm model equations. This isotherm gives the relationship between the equilibrium concentration of Ni ion on the solid phase and in the liquid at constant temperature.

4.1. Langmuir isotherm

The Langmuir isotherm is based on mono layer adsorption i.e. constant heat of adsorption for all sites, on the active sites of the adsorbent [34]. The data on the uptake of Ni^{2+} ion has been processed in accordance with the Langmuir isotherm equation

$$q_e = \frac{\left(Q_{max} bC_e\right)}{\left(1 + bC_e\right)} \tag{6}$$

The Langmuir isotherm in the linear form is as follows:

$$\left(\frac{C_e}{q_e}\right) = \left(\frac{C_e}{Q_{max}}\right) + \left(\frac{1}{\left(bQ_{max}\right)}\right) \tag{7}$$

where C_e is equilibrium concentration of Ni^{2+} ion in the solution (mg L^{-1}), q_e is amount of Ni^{2+} ion adsorbed at equilibrium (mg g^{-1}), Q_{max} is Maximum amount of Ni ion required to form a mono layer, i.e. adsorption capacity of the adsorbent (mg g^{-1}), b is Equilibrium constant representing adsorption intensity (L mg^{-1}). A plot is drawn for (C_e/q_e) Vs C_e. Q_{max} and b values can be calculated from the slope and intercept of the plot.

4.2. Freundlich isotherm

Based on the assumption that active sites are spread exponentially with respect to the heat of adsorption, the derivation of Freundlich isotherm was done. Based on the multilayer adsorption (heterogeneous surface), the Freundlich isotherm gives the equivalence between equilibrium liquid and solid phase capacity [35]. The Freundlich isotherm equation is given by:

$$q_e = K_f \left(C_e\right)^{1/n} \tag{8}$$

The following equation gives the linear form of the Freundlich isotherm:

$$log q_e = log K_f + \left(\frac{1}{n}\right) log C_e \tag{9}$$

where K_f (mg g^{-1}) and n (g L^{-1}) are Freundlich isotherm constants relating multilayer adsorption capacity and adsorption intensity for given adsorbate and adsorbent at a particular temperature. A plot is drawn for log q_e vs. log C_e. The n and K_f values are calculated from the slope and intercept of the plot. The isotherm constants along with the regression coefficients are listed in Table 5. From Figue 5, the q_e values predicted by the Langmuir model were close to the experimental values and therefore, Langmuir isotherm model fits to the adsorption of Ni^{2+} ion onto activated carbon sourced from CCP.

Table 5
Langmuir and Freundlich parameters for adsorption of nickel ion

Temperature (°C)	Langmuir constants			Freundlich constants		
	Q_{max} (mg g^{-1})	b (L mg^{-1})	R^2	K (mg g^{-1})	n (g L^{-1})	R^2
30	13.5	0.11	0.993	1.65	1.55	0.992

5. Kinetic studies

To analyse the adsorption rates of Ni ions on to AC from *Citrullus colocynthis*, pseudo first order and second order equations were tested.

5.1. Pseudo first order equation

The first equation which was proposed for the adsorption of adsorbate on the adsorbent based on the adsorbent capacity was given by Lagergren's pseudo first order equation [36] and it is given as

$$\frac{dq_t}{dt} = k_1\left(q_e - q_t\right) \tag{10}$$

This equation can be integrated for the boundary conditions $t = 0$, $q_t = 0$ and $t = t$, $q_t = q_t$ to give

$$log\left(q_e - q_t\right) = log\left(q_e\right) - k_1 t \tag{11}$$

where q_t is the amount of adsorbate on the surface adsorbent at any time t (min), q_e is the amount of adsorbate on the surface of adsorbent at equilibrium and k_1 is the equilibrium rate constant of pseudo first order adsorption. The constants k_1 and q_e is calculated from the slope of $\log(q_e - q_t)$ against time.

5.2. Pseudo second order model

The set of experimental readings were analysed with pseudo-second order equation [37]. The kinetic rate equation is

$$\frac{dq_t}{dt} = k_2\left(q_e - q_t\right)^2 \tag{12}$$

On integrating the above equation and applying the boundary conditions $t = 0$, $q_t = 0$ and $t = t$, $q_t = q_t$ and rearranging it obtain the linearized equation as

$$\frac{t}{q_t} = \frac{1}{h} + \frac{t}{q_e} \tag{13}$$

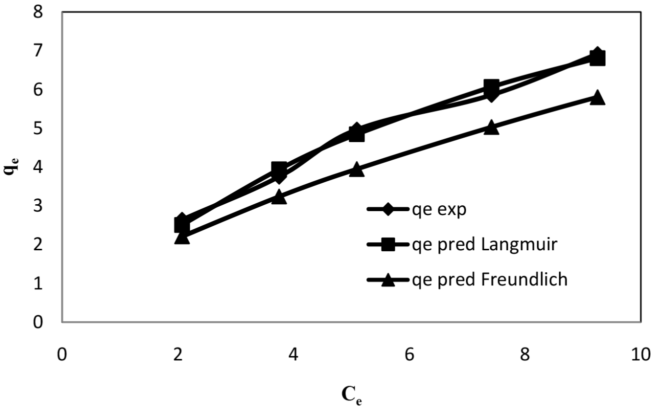

Fig. 5. Adsorption isotherm, experimental and predicted by Langmuir and Freundlich models at temperature = 30°C, carbon loading = 0.3 g (100 mL)$^{-1}$, pH = 6, time = 150 min.

Table 6
Comparison of pseudo-first order and pseudo-second order adsorption rate constants

Temperature (°C)	Pseudo-first order kinetics			Pseudo-second order kinetics			q_e (expt)
	q_e (mg g^{-1})	K_1 (min^{-1})	R^2	q_e (mg g^{-1})	K_2 (g mg^{-1}min^{-1})	R^2	(mg g^{-1})
30	2	0.011	0.902	5	0.0699	0.998	4.96914

Table 7
Comparison of the adsorption capacity of different adsorbents for Ni

Adsorbents	Adsorption capacity (mg g^{-1})	Reference
Activated carbon Moringa oleifera	19.084	[38]
Coir pith carbon	62.5	[39]
Granular activated carbon	1.49	[40]
Hazelnut husk AC (20°C)	5.757	[41]
Hazelnut husk AC (3°C)	7.181	[42]
Hazelnut husk AC (40°C)	10.107	[41]
Hazelnut husk AC (50°C)	11.64	[41]
Hevea brasiliensis	17.21	[42]
Parthenium	54.35	[43]
Peanut hull carbon	53.65	[40]
Pomegranate peel	52.20	[44]
Citrullus colocynthes peel	13.5	This study

where $h = k_2 q_e^2$, k_2 is the pseudo second order rate constant and h is the initial sorption rate. The equation constants can be determined by plotting t/q_t against t. Based on the regression coefficient and calculated values of adsorption capacity the adsorption process was found to obey the pseudo second order kinetics as shown in Table 6. Comparison of the adsorption capacity of different adsorbents for Ni is given in Table 7.

6. Development of regression model equation

In the present study, CCRD for four variables (adsorbent concentration, adsorbate concentration, pH, time), each with five levels (± 1 for the factorial points, 0 for the centre points and ± α for the axial points), was used as the experimental design model. This model has the advantage that it permits the use of relatively few combinations of variables for determining the complex response function [45]. A total of 30 experiments were required to be performed to calculate 15 coefficients of the second order polynomial equation. The adsorption of Ni^{2+} ion estimated as adsorption capacity was taken as the response of the system. The adsorption capacities and the design matrix derived experimentally using CCRD are shown in Table 8.

Based on the highest order polynomials which has the additional terms as significant according to the sequential model sum of squares, the selection of models were done. For percentage adsorption of Ni^{2+} ions, the quadratic model was suggested by the software, which was selected in this case due to the higher order polynomial. The coefficient of the model for the response was estimated using multiple regression analysis technique included in the RSM. The quadratic model thus obtained was given as follows:

Table 8
Measured and predicted response for adsorption of nickel using central composite rotary Design

Run order	Factors				Response (Y)	
	A	B	C	D	Predicted	Actual
1	0.2	25	4	60	5.97772	5.8934
2	0.4	15	4	60	1.91301	1.97526
3	0.3	20	6	90	4.78050	4.793147
4	0.2	30	8	120	9.74962	9.70812
5	0.2	25	4	120	6.69334	6.6326
6	0.4	15	8	60	3.23568	3.25038
7	0.4	25	4	120	3.63469	3.73606
8	0.2	15	8	60	5.55141	5.45004
9	0.4	15	8	120	3.36142	3.44574
10	0.3	20	6	90	4.78050	4.793147
11	0.3	20	10	90	6.43340	6.482747
12	0.3	20	6	90	4.86577	4.793147
13	0.3	20	6	30	4.17516	4.251067
14	0.1	20	6	90	8.89291	9.22616
15	0.3	10	6	90	2.51965	2.575653
16	0.5	20	6	90	3.51852	3.213808
17	0.3	20	6	150	5.01653	4.969147
18	0.3	20	6	90	4.86577	4.793147
19	0.3	30	6	90	6.56346	6.56712
20	0.3	20	2	90	3.08916	3.068347
21	0.2	15	4	60	4.07836	3.93996
22	0.4	15	4	120	2.18273	2.23926
23	0.2	25	4	120	6.66157	6.6326
24	0.2	25	8	60	8.14326	8.0582
25	0.4	25	4	60	3.36932	3.4747
26	0.3	20	6	90	4.74873	4.793147
27	0.4	15	8	60	3.20390	3.25038
28	0.3	20	6	90	4.74873	4.793147
29	0.2	15	8	120	6.12742	5.97276
30	0.4	25	8	120	5.50587	5.61574

$$\begin{aligned}
&Adsorption\ capacity(Y) = +1.85441 - 25.85623A + \\
&0.27391B + 0.19485C + 0.042695D + 33.6782A^2 \\
&-3.16395E-003B^2 - 6.08063E-003C^2 - 7.29792E \\
&-0005D^2 - 2.02187E-004BD - 8.96818E-004CD
\end{aligned} \tag{14}$$

A positive sign in front of the term indicates a synergistic effect and a negative sign is an indication for an antagonistic effect. The quality of the model developed was evaluated based on the correlation coefficient value (i.e.) the R^2 values in Table 9. It can be inferred that there is good agreement between experiment and model predicted values for relatively high values of R^2 (close to unity) as shown in Table 10 and Fig. 6. The standard deviation value should be smaller for better modeling as it gives closer predicted and actual values of the response and this indicates that the predicted value for Y is more accurate and closer to the actual value. The Model F-value of 1604.23 implies the model is significant. The chance of occurrence of large F-value is only 0.01% chance due to noise. "Prob > F" which has values less than 0.0500 indicates that the terms are significant. In this case A, B, C, D, AB, AD, BC, CD, A^2, B^2, D^2 are significant model terms. Values greater than 0.1000 indicate the model terms are not significant.

Table 9
Standard deviation and R^2 for the quadratic model equation

Std. Dev.	0.068	R-Squared	0.9993
Mean	4.95	Adj R-Squared	0.9987
C.V. %	1.38	Pred R-Squared	0.9965
PRESS	0.37	Adeq Precision	161.884

7. Interaction effects of adsorption variables

The three dimensional response surface plots were visualized to study the adsorption capacities of the present adsorbent over different combination of independent variables (Figs. 7a–f). These plots were drawn as a function of two factors and holding other two factors as constant. The optimum adsorption variables were obtained through point prediction method and surface response plot and are given in Table 11. Adsorption experiment was carried out at these conditions and the results were found to be well represented by the present model Eq. (14).

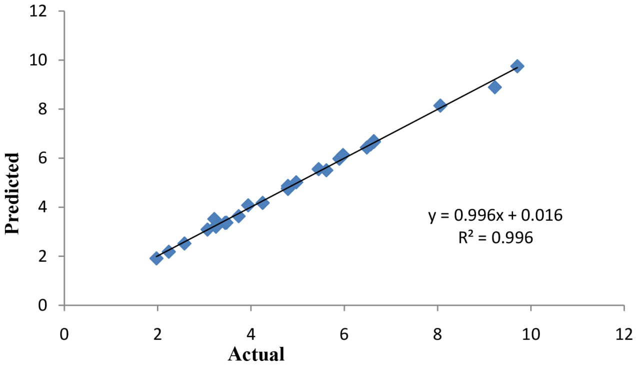

Fig. 6. Comparison between experimental and model predicted adsorption capacity using CCRD.

Table 10
Analysis of variance (ANOVA) for response surface quadratic model for adsorption capacity

Analysis of variance table [Partial sum of squares - Type III]						
Source	Sum of Squares	df	Mean Square	F Value	p-value	
					Prob> F	
Model	105.15	14	7.51	1604.23	< 0.0001	significant
A-A	41.35	1	41.35	8831.58	< 0.0001	
B-B	23.72	1	23.72	5065.92	< 0.0001	
C-C	16.22	1	16.22	3465.19	< 0.0001	
D-D	1.02	1	1.02	216.81	< 0.0001	
AB	0.068	1	0.068	14.58	0.0017	
AC	3.946E-003	1	3.946E-003	0.84	0.3731	
AD	0.17	1	0.17	36.81	< 0.0001	
BC	0.38	1	0.38	81.77	< 0.0001	
BD	9.449E-003	1	9.449E-003	2.02	0.1759	
CD	0.029	1	0.029	6.24	0.0246	
A^2	3.03	1	3.03	646.38	< 0.0001	
B^2	0.18	1	0.18	37.65	< 0.0001	
C^2	0.016	1	0.016	3.37	0.0862	
D^2	0.12	1	0.12	24.58	0.0002	
Residual	0.070	15	4.682E-003			
Lack of Fit	0.055	8	6.821E-003	3.05		
Pure Error	0.016	7	2.237E-003			
Cor Total	105.22	29				

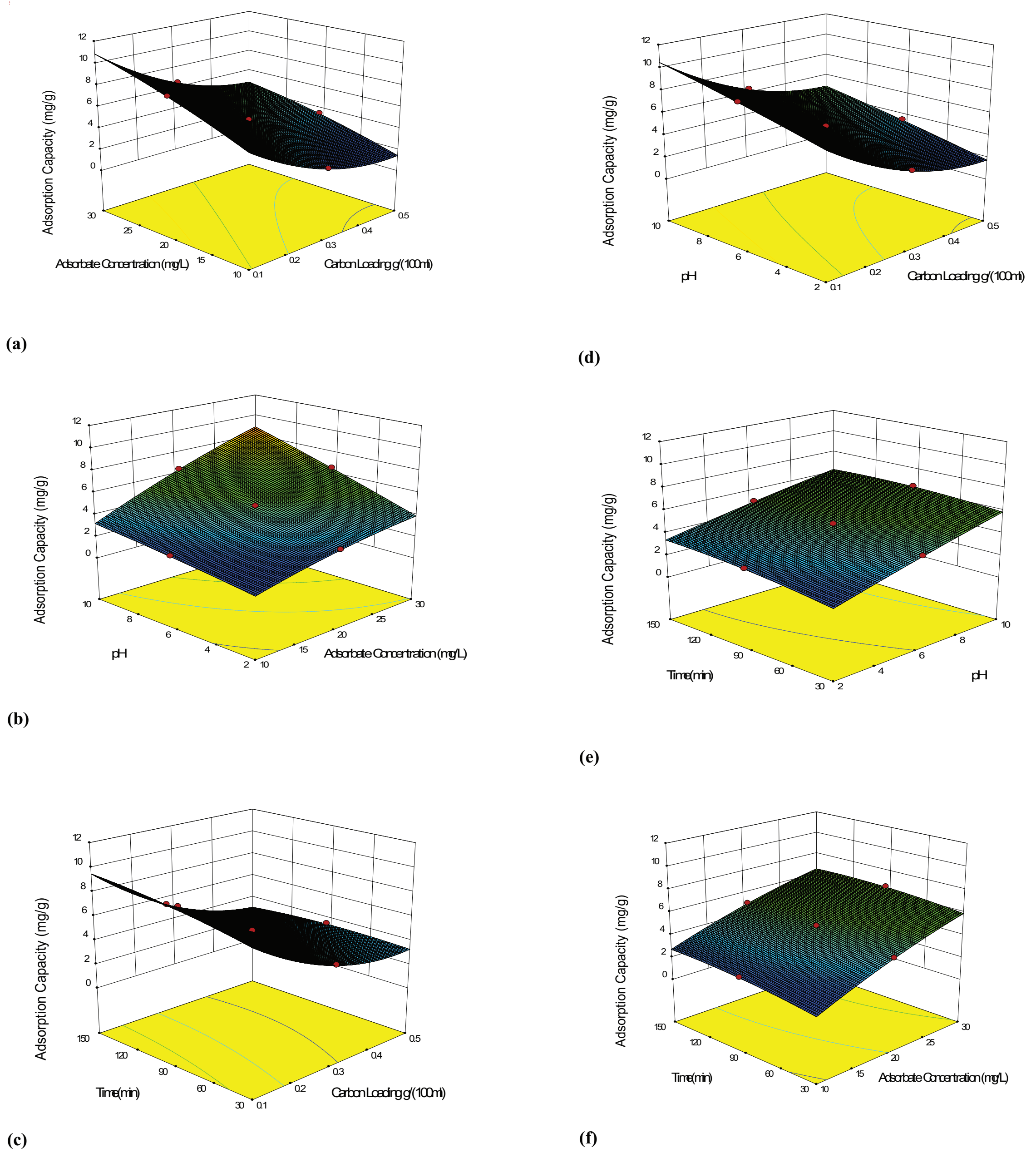

Fig. 7. ((a)–(f)) 3D Contour plots at carbon loading = 0.3 g, initial adsorbate concentration = 20 mg L^{-1}, pH = 6, time = 90 min, and temperature = 30°C.

Table 11
Optimized process variable values for adsorption process

Carbon loading (g (100 mL)$^{-1}$)	0.35
Initial Ni ion concentration (mg L^{-1})	25
pH	6
Adsorption time (min)	90
Temperature (°C)	30
Adsorption capacity (mg g^{-1})	
Predicted	6.25
Experimental	6.3864

8. Conclusion

AC produced from bio mass residue *Citrullus colocynthis* peel (CCP) was found to be effective for the adsorption of Ni^{2+} ion from the aqueous solution. The optimum pH was found to be 6. Isotherm studies were carried out using Langmuir and Freundlich equation of which Langmuir equation fitted the experimental well. The adsorption of Ni^{2+} ion onto AC was found to follow pseudo second order model. Response surface methodology is found to be useful software for the prediction of surface methodology and the central composite rotary design were used for the optimization of Ni^{2+} ions adsorption. The optimal results obtained from RSM were Initial adsorbate concentration 20 mg L^{-1}, carbon loading 0.3 (g (100 mL)$^{-1}$), pH 6, adsorption time 90 min and temperature 30°C. Under these conditions the adsorption capacity were found to closely match with the experiment and predicted values. Thus in this study, AC produced from CCP was found to be a suitable adsorbent for the removal of Ni^{2+} ion from synthetic waste water solution.

Symbols

A, B, C, D — Coded independent variable
$AB, AD, BC, CD, A^2, B^2, D^2$ — Significant model terms
C_o — Initial Ni^{2+} ion concentration in the solution (mg L^{-1})
C_e — Concentration of Ni^{2+} ion in the solution at equilibrium time (mg L^{-1})
F — Number of points
M — Mass of the adsorbent (g)
q_e — Adsorption capacity at equilibrium time (mg g^{-1})
V — Volume of the solution (L)
x_i — Dimensionless coded value of the i^{th} variable
X_i — Natural value of the i^{th} variable
Y — Particular response evaluated
Y_i — Predicted response

Greek

α — Number of points in the factorial portion of the design for rotatability
β_i — i^{th} linear variable coefficient
β_{ij} — ij^{th} interaction coefficient
$\beta_0, \beta_1, \beta_2, \beta_3, \beta_4, \beta_{11}, \beta_{22}, \beta_{33}, \beta_{44}, \beta_{12}, \beta_{13}, \beta_{14}, \beta_{23}, \beta_{24}, \beta_{34}$ — Regression coefficients

Abbreviations

AC — Activated Carbon
CAC — Commercial Activated Carbon
ANOVA — Analysis of Variance
CCP — *Citrullus colocynthis* Peel
CCRD — Central Composite Rotatable Design
EEC — Euro Environmental Contracts
pH — Potential of Hydrogen
RSM — Response Surface Methodology
pH_{ZPC} — pH Point of Zero Charge
WHO — World Health Organization

References

[1] A.H. Hawari, C.N. Mulligan, Heavy metals uptake mechanisms in a fixed bed column by calcium-treated anaerobic biomass, Process Biochem., 41 (2006) 187–198.

[2] F. Qin, B. Wen, X.Q. Shan, Y.N. Xie, T. Liu, S.Z. Zhang, S.U. Khan, Mechanisms of competitive adsorption of Pb, Cu, and Cd on peat, Environ. Pollut., 144 (2006) 669–680.

[3] WHO's Guidelines for Drinking-water Quality, set up in Geneva, 1993.

[4] L. Canet, M. Ilpide, P. Seta, Efficient facilitated transport of lead, cadmium, zinc and silver across a flat sheet-supported liquid membrane mediated by lasalocid, Separ. Sci. Technol., 37 (2002) 1851–1860.

[5] G. Yan, T. Viraraghavan, Heavy metal removal in a biosorption column by immobilized M. Rouxii biomass, Bioresour Technol., 78 (2001) 243–249.

[6] K. Kadirvelu, K. Thamaraiselvi, C. Namasivayam, Removal of heavy metals from industrial waste waters by adsorption onto activated carbon prepared from an agricultural solid waste, Bioresour Technol., 76 (2001) 63–65.

[7] F. Ruggieri, A.A. D'Archivio, D. Di Camillo, L. Lozzi, M.A. Maggi, R. Mercorio, S. Santucci, Development of molecularly imprinted polymeric nano fibers by electro spinning and applications to pesticide adsorption, J. Separ. Sci., 38 (2015) 1402–1410.

[8] Y. Zhang, S. Yuan, X. Feng, H. Li, J. Zhou, B. Wang, Preparation of nano fibrous metal–organic framework filters for efficient air pollution control, J. Amer. Chem. Soc., 138 (2016) 5785–5788.

[9] C.K. Lee, K.S. Low, Removal of copper from solution using moss, Environ. Sci. Technol. Lett., 10 (1989) 395–404.

[10] W.T. Tan, S.T. Ooi, C.K. Lee, Removal of chromium (VI) from solution by coconut husk and palm pressed fibres, Environ. Technol., 14 (1993) 277–282.

[11] I. Saucedo, E. Guibal, C.H. Roulph, P. Cloirec, Sorption of uranyl ions by a modified chitosan: kinetic and equilibrium studies, Environ. Technol., 13 (1992) 1101–1105.

[12] E. Munaf, R. Zein, R. Kurniadi, I. Kurniadi, The use of rice husk for removal of toxic metals from waste water, Environ. Technol., 18 (1997) 359–362.

[13] T.W. Tee, A.R.M. Khan, Removal of lead, cadmium and zinc by waste tea leaves, Environ. Technol., 9 (1988) 1223–1232.

[14] H. Hasar, Y. Cuci, Removal of Cr (VI), Cd (II), and Cu (II) by using AC prepared from almond husk, Environ. Technol., 21 (2000) 1337–1342.

[15] S. Jenifer, M. Srihari, V. Shanmugam, M.H. Kalavathy, L.R. Miranda, Production of activated carbon from biomass residues, Int. J. Bioprocess Technol., 1 (2014) 1.

[16] J.N. Sahu, J. Acharya, B.K. Sahoo, B.C. Meikap, Optimization of lead (II) sorption potential using developed activated carbon from tamarind wood with chemical activation by zinc chloride Desal. Water Treat., 57 (2016) 2006–2017.

[17] K.N. Aboua, Y.A. Yobouet, K.B. Yao, D.L. Gone, A. Trokourey, Preparation of effective TiO_2/Bi_2O_3 photo catalysts for water treatment, J. Environ. Manage., 156 (2015) 10–15.

[18] M.H. Kalavathy, T. Karthikeyan, S. Rajagopal, L.R. Miranda, Kinetic and isotherm studies of Cu(II) adsorption onto H_3PO_4-activated rubber wood saw dust, J. Colloid Interface Sci., 292 (2005) 354–362.

[19] M. Kincl, S. Turk, F. Vrecer, Application of experimental design methodology in development and optimization of drug release method, Int. J. Pharmaceutics, 291 (2005) 39–49.

[20] M. Rahmani, E. Ghasemi, M. Sasani, Application of response surface methodology for air assisted-dispersive liquid-liquid micro extraction of deoxynivalenol in rice samples prior to HPLC-DAD analysis and comparison with solid phase extraction cleanup, Talanta, 165 (2017) 27–32.

[21] A.A. D'Archivio, M.A. Maggi, F. Ruggieri, Prediction of the retention of s-triazines in reversed-phase high-performance liquid chromatography under linear gradient-elution conditions, J. Separ. Sci., 37 (2014) 1930–1936.

[22] A.A. D'Archivio, M.A. Maggi, F. Ruggieri, M. Carlucci, V. Ferrone, G. Carlucci, Optimization by response surface methodology of micro extraction by packed sorbent of non steroidal anti-inflammatory drugs and ultra-high performance liquid chromatography analysis of dialyzed samples, J. Pharm. Biomed. Anal., 125 (2016) 114–121.

[23] A.A. D'Archivio, M.A. Maggi, C. Marinelli, F. Ruggieri, F. Stecca, Optimization of temperature-programmed gas chromatographic separation of organochloride pesticides by response surface methodology, J. Chromatography A, 1423 (2015) 149–157.

[24] D.C. Montgomery, Design and analysis of experiments, fifth edition, John Wiley & Sons, New York. 2001

[25] G.M. Clarke, R.E. Kempson, Introduction to the Design and Analysis of Experiments, Arnold, London. 1997

[26] J.A. Cornell, How to apply response surface methodology, second edition, American Society for Quality Control, Wisconsin. 1990

[27] G. Box, N. Draper, Empirical model building and response surfaces, John Wiley & Sons, New York. 1987

[28] Z.R. Holan, B. Volesky, Biosorption of lead and $Ni^{2+}$by biomass of marine algae, Biotechnol. Bioeng., 43 (1994) 1001–1009.

[29] R. Wachter, A. Cordery, Response surface methodology modeling of diamond like carbon film deposition, Carbon, 37 (1999) 1529–1537.

[30] Rivera –Utrilla I Bautista-Toledo, M.A. Ferro-García, C. Moreno-Castilla method, Activated carbon surface modifications by adsorption of bacteria and their effect on aqueous lead adsorption, J. Chem. Technol. Biotechnol., 76 (2001) 1209–1215.

[31] D.E. Egirani, A.R. Baker, J.E. Andrews, Copper and zinc removal from aqueous solution by mixed mineral systems: I. Reactivity and removal kinetics, J. Colloid Interface Sci., 291 (2005) 319–325.

[32] V.C. Srivatsava, I.D. Mall, I.M. Mishra, Adsorption of toxic metal ions onto activated carbon: Study of sorption behaviour through characterization and kinetics, Chem. Eng. Process: Process Intensif., 47 (2008) 1269–1280.

[33] I. Aloma, M.A. Martin-Lara, I.L. Rodriguez, G. Blazquez, M. Calero, Removal of nickel(II) ions from aqueous solutions by biosorption on sugarcane bagasse, J. Taiwan Inst. Chem. Eng., 43 (2012) 275–281.

[34] I. Langmuir, The adsorption of gases on plane surfaces of glass, mica and platinum, J. Amer. Chem. Soc., 40 (1918) 1361–1403.

[35] H.Z. Freundlich, Uber die. Adsorption. in. losungen, Zeitschrift fur Physical Chemistry, 57 (1906) 385–470.

[36] S. Lagergren, Zur theorie der sogenannten adsorption gelöster stoffe, Kungliga Svenska Vetenskapsakademiens, Handlingar, 24 (1898) 1–39.

[37] Y.S. Ho, G. McKay, The kinetics of sorption of basic dyes from aqueous solution by sphagnum moss peat, Canad. J. Chem. Eng., 76 (1998) 822–827.

[38] M.H. Kalavathy, L.R. Miranda, M. Oleifera, A solid phase extractant for the removal of copper, nickeland zinc from aqueous solutions, Chem. Eng. J., 158 (2010) 188–199.

[39] K. Kadirvelu, K. Thamaraiselvi, C. Namasivayam, Adsorption of nickel(II) from aqueous solution onto activated carbon prepared from coir pith, Separ. Purif. Technol., 24 (2001) 497–505.

[40] K. Periasamy, C. Namasivayam, Removal of nickel(II) from aqueous solution wastewater using an agricultural waste: peanut hulls, Waste Manage., 15 (1995) 63–68.

[41] E. Dermibas, M. Kobya, S. Oncel, S. Sencan, Removal of Ni (II) from aqueous solution by adsorption onto hazelnut shell activated carbon: equilibrium studies, Bioresour Technol., 84 (2002) 291–293.

[42] H. Kalavathy, B. Karthik, L.R. Miranda, Removal and recovery of Ni and Zn from aqueous solution using activated carbon from Hevea brasiliensis: batch and column studies, Colloids Surfaces B, 78 (2010) 291–302.

[43] K. Kadirvelu, P. Senthilkumar, K. Thamaraiselvi, V. Subburam, Activated carbon prepared from biomass as adsorbent: elimination of Ni (II) from aqueous solution, Bioresourc Technol., 81 (2002) 87–90.

[44] A. Bhatnagara, A.K. Minochaa, Biosorption optimization of Nickel removal from water using Punica granatum peel waste, Colloids Surf. B Biointerfaces, 76 (2010) 544–548.

[45] C.A. Toles, W.E. Marshall, M.M. Johns, Granular activated carbon from nutshells for the uptake of metal ions and organic compounds, Carbon, 35 (1999) 1407–1414.